# Fine-Tuning of the Binding and Dissociation of CO by the Amino Acids of the Heme Pocket of *Coprinus cinereus* Peroxidase[†]

Alessandro Feis,[‡] Elisa Santoni,[‡] Francesca Neri,[‡] Chiara Ciaccio,[§] Giampiero De Sanctis,[||] Massimo Coletta,[§] Karen G. Welinder,[⊥] and Giulietta Smulevich*[,‡]

*Dipartimento di Chimica, Universita' di Firenze, Polo Scientifico, Via della Lastruccia 3, I-50019 Sesto Fiorentino (FI), Italy, Dipartimento di Medicina Sperimentale e Scienze Biochimiche, Università di Roma Tor Vergata, Via Montpellier 1, I-00133 Roma, Italy, Dipartimento di Biologia Molecolare, Cellulare ed Animale, Università di Camerino, I-62032 Camerino (MC), Italy, and Institut for Bioteknologi, Aalborg Universitet, Sohngaardsholmsvej 49, DK-9000 Aalborg, Denmark*

*Received May 28, 2002; Revised Manuscript Received August 28, 2002*

ABSTRACT: Resonance Raman and infrared spectra and the CO dissociation rates ($k_{off}$) were measured in *Coprinus cinereus* peroxidase (CIP) and several mutants in the heme binding pocket. These mutants included the Asp245Asn, Arg51Leu, Arg51Gln, Arg51Asn, Arg51Lys, Phe54Trp, and Phe54Val mutants. Binding of CO to CIP produced different CO adducts at pH 6 and 10. At pH 6, the bound CO is H-bonded to the protonated distal His55 residue, whereas at alkaline pH, the vibrational signatures and the rate of CO dissociation indicate a distal side which is more open or flexible than in other plant peroxidases. The distal Arg51 residue is important in determining the rate of dissociation in the acid form, increasing by 8−17-fold in the Arg51 mutants compared to that for the wild-type protein. Replacement of the distal Phe with Trp created a new acid form characterized by vibrational frequencies and $k_{off}$ values very similar to those of cytochrome *c* peroxidase.

Carbon monoxide is a sensitive probe for investigating both proximal ligand properties and distal environmental effects in the heme cavity of heme proteins. In particular, polar interactions and the formation of H-bonds between the bound CO and the distal residues increase the extent of back-donation from the Fe $d_\pi$ to the CO $\pi^*$ orbitals. As a consequence, the Fe−C bond strengthens while the CO bond weakens, thereby increasing the $\nu_{FeC}$[1] vibrational frequencies and decreasing the $\nu_{CO}$ frequencies (*1*, *2*). For a large class of CO adducts of heme proteins and of model compounds containing an imidazole as the fifth ligand, a linear correlation between the frequencies of the $\nu_{FeC}$ and $\nu_{CO}$ stretching modes has been found. The correlation plots have a negative slope and depend on the extent of $\pi$ back-bonding (*1*−*3*). This relationship has a counterpart in the study of the kinetics of CO dissociation, which is fairly sensitive to the electronic environment of the bound CO as well as to the stereochemical situation of the heme surroundings. Uno and co-workers (*4*) noted an inverse linear relationship between log $k_{off}$ and $\nu_{FeC}$ for several heme proteins and concluded that the rate of CO dissociation is determined by Fe−C bond strength, which is, in turn, modulated by local polarity and H-bonding. Vibrational spectroscopy can be successfully exploited in the characterization of CO complexes, since many previous studies provide a solid framework for correlating the stretching frequencies of the CO and FeC bonds with structural properties (*2*). Moreover, the CO signatures can be readily assigned upon isotopic substitution by measuring spectra for both $^{12}$CO and $^{13}$CO adducts.

In previous studies of CO adducts of HRPC (*5*) and CCP (*6*), it was found that in these peroxidases at acidic pH the oxygen atom of the bound CO experienced stronger H-bond interactions with the distal residues than in myoglobin. In particular, HRPC displays two conformers, one H-bonded with the distal Arg (form I) and the other with the distal His (form II), whereas CCP is characterized by only one form in which the CO molecule is H-bonded to the distal Arg via a water molecule. Concomitantly, the CO dissociation rate of these peroxidase complexes was found to be 100-fold slower than that of myoglobin (*7*, *8*). However, it should be noted that a single rate of CO dissociation was found for

[†] This work was supported by the Italian Consiglio Nazionale delle Ricerche (CNR) (G.S.), the Ministry of Education, Universities, and Research (MIUR) (PRIN MM03185591) (G.S. and M.C.), the EU Biotechnology Program "Towards Designer Peroxidases" (BIO4-CT97-2031) and the EU Human Capital and Mobility Programme "Peroxidases in Agriculture, the Environment and Industry" (Contract FMRX-CT98-0200) (G.S. and K.G.W.). We acknowledge the COST Action D21 "Metallo Enzymes and Chemical Biomimetics" for supporting the exchange among the different laboratories.

* To whom correspondence should be addressed. Telephone: +39 055 4573083. Fax: +39 055 4573077. E-mail: giulietta.smulevich@unifi.it.

[‡] Universita' di Firenze.

[§] Università di Roma Tor Vergata.

[||] Università di Camerino.

[⊥] Aalborg Universitet.

[1] Abbreviations: RR, resonance Raman; IR, infrared; HRPC, horseradish peroxidase isoenzyme C; CIP, *C. cinereus* peroxidase, expressed in *Aspergillus oryzae* (identical to ARP, *A. ramosus* peroxidase); CCP, cytochrome *c* peroxidase; CCP(MI), recombinant cytochrome *c* peroxidase carrying N-terminal Met and Ile; $\nu_{FeC}$, Fe−C stretching vibrational mode; $\nu_{CO}$, C−O stretching vibrational mode; $\delta_{FeCO}$, Fe−C−O bending vibrational mode; wt, wild type; $k_{off}$, CO dissociation rate constant; $k_{on}$, CO association rate constant; $K_{CO}$, equilibrium CO binding constant.

10.1021/bi026203c CCC: $22.00 
Published on Web 10/11/2002

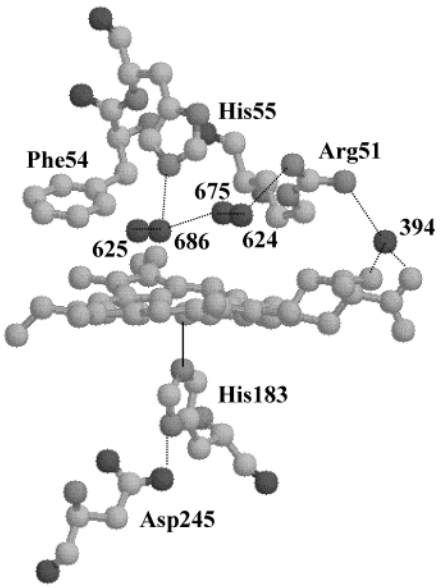


FIGURE 1: Structural diagram of the heme pocket of CIP according to the crystal structure of Kunishima et al. (*11*). Dotted lines represent hydrogen bonds inferred on the basis of distance criteria. Five observed water molecules are also shown (three-digit numbers).

HRPC, although the strength of the Fe−C bond is significantly different for the two conformers (*7*). Similar rates of CO dissociation were also observed for recombinant cytochrome *c* peroxidase (CCPMI) and selected mutants which, however, exhibit very different $\nu_{FeC}$ frequencies (*7*).

In the study presented here, we monitor the CO ligation state of CIP and selected mutants in which residues capable of interacting with the heme group, via its ligands on both the proximal and distal sides, were replaced. The crystal structures of CIP and the *Arthromyces ramosus* peroxidase (which have been shown to be identical) (*9*) have been determined (*10*, *11*). The environment of the heme is shown in Figure 1. The iron is coordinated to His183 on the proximal side which in turn is H-bonded to an Asp side chain (Asp245) that is invariant in the peroxidase superfamily. On the distal side, the catalytically important amino acids, His55 and Arg51, are conserved in all peroxidases and form an extended H-bond network with water molecules. Furthermore, Arg51 is linked to oxygen atoms of the propionate groups of the heme via a water molecule. On the distal side, a Phe (Phe54) is also present as in HRPC, while in CCP, this position is occupied by a Trp residue. Upon comparison of the structure of CIP (*11*) with those of HRPC (*12*) and CCP (*13*), it appears that the guanidinium group of the Arg residue is located farther away from the iron atom than in HRPC and CCP, whereas the phenyl ring is closer and approximately 3.3−3.5 Å above the heme plane. Previous results obtained for the ferric and ferrous forms of distal variants of CIP at the Arg (*14*) and Phe (*15*) positions have shown that these residues are important not only in maintaining the architecture of the heme cavity but also for the stabilization of the anionic ligand binding. In this work, we report the results obtained from spectroscopic observation on the CO-bound forms and those obtained from kinetic and equilibrium measurements on the CO adducts of wild-type (wt) CIP and selected mutants. These data are compared with those reported for other peroxidases in the context of their crystal structures.

## MATERIALS AND METHODS

The procedure for the production of CIP and its mutants has been described elsewhere (*16*−*18*). All the CIP mutants are active. The Asp245 and Phe51 mutants behave in a manner very similar to that of the wt protein, whereas the Arg51 mutants required an at least 5-fold excess of hydrogen peroxide for complete formation of compound I (K. G. Welinder, personal communication).

The following buffers were used: 0.05 M citric acid-sodium citrate (pH 4−5.5), 0.1−0.01 M sodium phosphate (pH 5.7−7), 0.05 bicine (pH 8.2), 0.25 M borate (pH 9), 0.2 M 3-(cyclohexylamino)-1-propanesulfonic acid (CAPS) or 0.05 M borate (pH 10), and 0.2 M sodium bicarbonate (pH 10.7). All experiments were performed at a constant ionic strength of 0.1 M adjusted using $K_2SO_4$. The pH was measured directly in the sample for RR, or in a portion of the samples for IR, after the measurements, by means of a microelectrode.

The CO complexes were prepared by first flushing the ferric protein solution with nitrogen, then flushing with $^{12}CO$ (Rivoira) or $^{13}CO$ (FluoroChem), and reducing the protein with a 5% volume addition of a fresh sodium dithionite (20 mg/mL) solution. Deuterated CIP−CO (complex of CIP and CO) was prepared by washing the protein in $D_2O$ and dissolving it in buffered $D_2O$ (99.8%, Merck) [0.5 M borate buffer (pD 10.2)]. The protein was then flushed with CO and reduced with sodium dithionite in $D_2O$.

The protein concentrations were 30−60 $\mu$M for the RR samples, 70−180 $\mu$M for the electronic absorption spectra, and ∼580 $\mu$M for the IR samples.

The RR spectra were obtained by excitation with the 413.1 nm line of a $Kr^+$ laser (Coherent, Innova 302). The backscattered light from a slowly rotating NMR tube was collected and focused into a double monochromator (Jobin-Yvon HG2S 2000), equipped with a cooled photomultiplier (RCA C31034A). The power at the sample was 1.5−5 mW. The RR spectra in the $\nu_4$ mode region were checked to ensure that the amount of five-coordinated ferrous species due to laser photolysis was small enough not to appreciably contribute to the RR spectra in the low-frequency region. The measurement range was 380−630 $cm^{-1}$, although Figures 2, 4, 6, and 7 display only the 450−630 $cm^{-1}$ range for graphical reasons. The RR spectra were calibrated with the intense low-frequency bands of indene and $CCl_4$ to an accuracy of 1 $cm^{-1}$ for isolated bands.

Peak intensities and positions of the IR and RR spectra of the Arg51Asn−CO adduct (Table 2) and RR spectra of the Phe54Trp−CO adduct were determined by a curve-fitting program. For the latter, best fits were obtained using Lorentzian line shapes with a bandwidth of 16 $cm^{-1}$.

Electronic absorption spectra were recorded at room temperature (23 ± 1 °C) with a double-beam Cary 5 spectrometer. Fourier transform infrared spectra were recorded at room temperature with a Bruker IFS120 IR spectrometer. The CO complexes were transferred with a gastight Hamilton syringe flushed with CO into a vacuum-tight $CaF_2$ infrared cell with a path length of 0.1 mm that had been flushed with CO. The spectra were recorded after evacuation of the sample chamber, and reference spectra of corresponding buffer solutions without protein were recorded.

Table 1: Vibrational Frequencies ($cm^{-1}$) and CO Dissociation Rate Constants ($k_{off}$, $\times 10^{-4}$ $s^{-1}$) of Ferrous-CO Complexes for CIP, HRPC, CCP, and Selected Mutants at Different pH Values

| | $\nu_{CO}$ ($cm^{-1}$) | $\Delta^{13}CO$ ($cm^{-1}$) | $\Delta D_2O$ ($cm^{-1}$) | $\nu_{FeC}$ ($cm^{-1}$) | $\Delta^{13}CO$ ($cm^{-1}$) | $k_{off}$ ($\times 10^4$ $s^{-1}$) | ref | numbering in Figure 11 |
|---|---|---|---|---|---|---|---|---|
| acidic forms | | | | | | | | |
| CIP | 1930.5 | | −1 | 519 | −5 | 0.45 ± 0.3 | this work | 8 |
| Asp245Asn | 1939.5 | | | 517 | −6 | 1.2 ± 0.1 | this work | 10 |
| Arg51Lys | 1934.5 | | | 514 | | 5.4 ± 0.7 | this work | 13 |
| Arg51Gln | 1933 | | | 518 | | 7.7 ± 0.9 | this work | 12 |
| Arg51Asn | 1932 | | | 519 | −3 | 0.45 ± 0.5 | this work | 8 |
| | 1942 | | | 506 | −3 | 7.8 ± 1.1 | this work | 18 |
| Arg51Leu | 1925 | −43 | | 533 | −5 | 0.42 ± 0.6 | this work | 2 |
| | 1943 | | | 519 | −6 | 3.8 ± 0.5 | this work | 6 |
| | 1938.5 | −44 | | 521 | −6 | 2.5 ± 0.4 | this work | 7 |
| Phe54Trp | 1919 | | | 528 | | 0.091 ± 1.8 | this work | 5 |
| | 1930 | | | 518 | | 0.76 ± 1.2 | this work | 9 |
| | 1942 | | | 508 | | 0.76 ± 1.2 | this work | 9 |
| Phe54Val | 1944 | | | 508 | | | this work | |
| HRPC (form I) | 1906 | | −2 | 539 | −4 | 1.1 | *5*, *19*, *22*, *26*, *28*, *32* | 1 |
| HRPC (form II) | 1933 | | −1 | 516 | −5 | 1.1 | *5*, *19*, *22*, *26*, *28*, *32* | 11 |
| HRPC (pH 3) | 1967 | | | 492 | | | *23* | |
| Arg38Leu | 1941.5 | | −1 | 515 | −5 | | *5*, *28* | |
| Phe41Val (form a) | 1912 | | −1 | 526 | −5 | | *33* | |
| Phe41Val (form b) | 1919 | | −1 | 519 | −5 | | *33* | |
| CCP | 1922 | | −2 | 530 | −5 | | *22*, *24* | |
| CCPMI | 1922 | | | 503 | | 0.7 | *6*, *7* | 21 |
| Arg48Leu | 1941 | | | 500 | −8 | 13.8 | *6*, *7* | 26 |
| Arg48Lys | 1936 | | | 510 | −6 | 3.7 | *6*, *7* | 14 |
| Trp51Phe | 1932 | | | 528 | −5 | | *6*, *7* | |
| Asp235Asn | 1933 | | | 531 | −5 | 0.8 | *6*, *7* | 3 |
| alkaline forms | | | | | | | | |
| CIP | 1951 | | | 503 | −3 | 63 ± 0.5 | this work | 23 |
| Asp245Asn | 1959 | | | 503 | −4 | 60 ± 0.6 | this work | 24 |
| Arg51Lys | 1948 | | | 507 | | 18 ± 0.3 | this work | 17 |
| | | | | | | 100 ± 0.2 (denatured) | this work | |
| Arg51Gln | 1947 | | | 502 | | 4.8 ± 0.6 | this work | |
| Arg51Asn | 1952 | | | 495 | −4 | 16 ± 0.3 | this work | 27 |
| | 1942 | | | 506 | −3 | 3.2 ± 0.5 | this work | 20 |
| Arg51Leu | 1956 | | | 503 | | | this work | |
| | 1925 | −43 | | 533 | −5 | 0.42 ± 0.6 | this work | 2 |
| Phe54Trp | 1956 | | | 503 | | 3.5 ± 0.5 | this work | 22 |
| HRPC | 1933 | | | 530 | | 4 | *5*, *19*, *28* | 4 |
| CCP | 1948 | | | 503 | | | *24* | |
| CCPMI | 1948 | | | 507 | −7 | 8 ± 0.1 | *6*, *7* | 16 |
| Arg48Leu | 1951 | | | 500 | −4 | 20 ± 0.2 | *6*, *7* | 25 |
| Arg48Lys | 1945 | | | 507 | −5 | 6.4 ± 0.1 | *6*, *7* | 15 |
| Asp235Asn | 1951 | | | 505 | −5 | 7 ± 0.1 | *6*, *7* | 19 |

Table 2: Spectral Parameters of the RR and IR Bands of the Arg51Asn−CO Adducts Obtained by a Band-Fitting Program Using Lorentzian Line Shapes[a]

| | RR $\nu_{FeC}$ | | | IR $\nu_{CO}$ | | |
|---|---|---|---|---|---|---|
| | $\bar{\nu}$ | $\Delta\bar{\nu}$ | $I$ (%) | $\bar{\nu}$ | $\Delta\bar{\nu}$ | $I$ (%) |
| pH 6 | 495 | 16 | 10.4 | | | |
| | 506 | 16 | 65.2 | 1942 | 17 | 67 |
| | 519 | 16 | 24.4 | 1932 | 17 | 33 |
| pH 10 | 495 | 16 | 27.3 | 1952 | 17 | 32 |
| | 506 | 16 | 55.3 | 1942 | 17 | 52 |
| | 519 | 16 | 17.2 | 1933 | 17 | 16 |

[a] Frequencies ($\nu$) and bandwidths ($\Delta\bar{\nu}$) are given in $cm^{-1}$. The band intensities ($I$) are in arbitrary units expressed as a percentage.

Equilibrium CO binding constants have been determined by injecting the desired volume of a CO aqueous solution into a gastight cuvette with a rubber stopper containing a solution of degassed protein, in the presence of sodium dithionite (20 mg/mL) and in the absence of the gas phase to avoid redistribution of the gas. The solution was equilibrated for 5 min under gentle shaking, and the spectra were recorded in the Soret region (between 370 and 450 nm). The titration curve was performed by several additions of CO, and it allowed us to determine the equilibrium constant according to the following relationship (valid at each wavelength):

$$Y = OD_x - OD_{unl}/(OD_{CO} - OD_{unl}) = K[CO]/(1 + K[CO]) \quad (1)$$

where $Y$ is the percentage of CO-bound species, $OD_x$ is the optical density at a given wavelength after the addition of CO, $OD_{unl}$ is the optical density of the reduced protein in the absence of CO, $OD_{CO}$ is the optical density of the CO-bound form, $K$ is the equilibrium constant, and [CO] is the concentration of free CO (calculated by subtracting the number of moles of CO-bound protein from the number of moles of CO added). All equilibrium isotherms displayed a hyperbolic form, as expected for a protein with only one heme site.

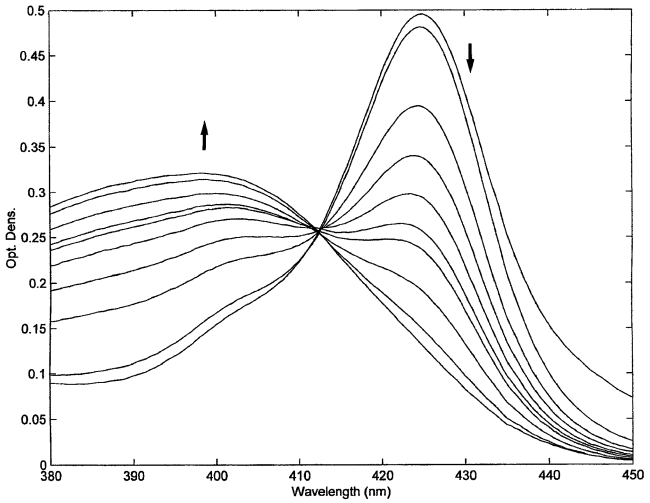


FIGURE 2: Conversion of CO-ferrous Arg51Leu mutant CIP to the ferric form in the presence of oxygen at pH 6.0. Traces were recorded at 0, 3, 20, 30, 40, 50, 60, 90, 130, and 200 min time intervals. The direction of the change in absorbance with time is indicated by arrows.

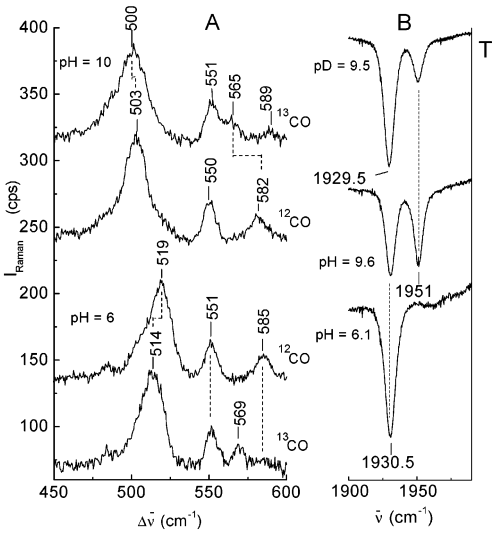


FIGURE 3: (A) RR spectra of the complexes of wt CIP at pH 10 and 6 with $^{13}$CO and $^{12}$CO. The spectra were measured with an excitation wavelength at 413.1 nm and a spectral resolution of 5 cm$^{-1}$. The integration times (from top to bottom) were 14, 20, 18, and 6 s/0.5 cm$^{-1}$; (B) IR spectra of wt CIP at pD 9.5, pH 9.6, and pH 6.1 with $^{12}$CO. Experimental conditions: 0.5 cm$^{-1}$ spectral resolution and 2000 scans accumulated.

CO dissociation kinetics were measured by injecting a concentrated solution of the proteins in the presence of a slightly substoichiometric amount of CO and of a minimum amount of sodium dithionite, into a 50-fold volume excess of an oxygenated buffer solution at the desired pH and at 20 °C. The obtained values are the average of at least three experiments, and the range of variability has always been below 10%. The absorption spectra were recorded in the Soret region (between 370 and 450 nm) at varying time intervals over a time range corresponding to 8−10 half-lives, as required by the spectral time evolution (see Figure 2 as an example), following the oxidation of the protein and checking that the oxidation is rate-limited by the CO dissociation process (*19*). The control was exerted by repeating the kinetic measurements under reducing conditions and using microperoxidase-8 as a CO trap (*19*, *20*); in all cases, the same kinetic constant was obtained, clearly indicating that the oxidation of the ferrous enzyme was much faster than the CO dissociation process and no oxyferrous peroxidase intermediate was observed. Moreover, the existence of an isosbestic point (Figure 2) indicates that intermediates in the oxidation of the ferrous enzyme, such as the ligand free ferrous enzyme and the ferrous−oxygen complex, do not accumulate at significant levels during the reaction. Therefore, only two populations are present, and the kinetics at one wavelength may be representative of the time course taking place at various wavelengths. The disappearance of the CO complex was monitored following the conversion of CO-ferrous to ferric protein at the absorption maximum of the CO-bound form (423−425 nm depending on the protein and pH), which corresponds to the maximum difference between the initial and final spectra (see Figure 2). wt CIP and the mutants behaved in the same way. Rate constants were obtained from least-squares fitting of data, employing one or two exponentials. The measurements have been carried out using a Jasco V-530 spectrophotometer.

## RESULTS AND DISCUSSION

*CIP−CO*. The CO complex of ferrous CIP is readily formed when CO is added. It is stable for several hours. The electronic absorption spectrum is very similar to those observed previously for other peroxidases (*21*) and is characterized by a Soret band at 425 nm and Q-bands at 542 and 572 nm. The spectrum does not change between pH 4 and 10 (data not shown).

Figure 3A shows the low-frequency region RR spectra of the wt CIP−CO complex at pH 6 and 10 in the presence of $^{12}$CO or $^{13}$CO. At pH 6, the strong band observed at 519 cm$^{-1}$ for the $^{12}$CO complex shifts down by 5 cm$^{-1}$ in the $^{13}$CO complex. This is accompanied by the shift of a weak band from 585 to 569 cm$^{-1}$. The band at 585 cm$^{-1}$ overlaps with a porphyrin mode, resulting in a residual intensity at this frequency in the spectrum of the $^{13}$CO complex. Similar results are observed at pH 10, where the strong band at 503 cm$^{-1}$ shifts to 500 cm$^{-1}$, and the band at 582 cm$^{-1}$ is observed at 565 cm$^{-1}$ in the $^{13}$CO spectrum. On the basis of the isotopic shifts, the bands at 519 and 503 cm$^{-1}$ are assigned to two $\nu_{FeC}$ stretching modes. The bands at higher frequencies, showing a large isotopic shift, are assigned to the corresponding $\delta_{FeCO}$ bending modes. The corresponding IR spectra are shown in Figure 3B. At pH 6, a single band at 1930.5 cm$^{-1}$ is observed. This band decreases in intensity at pH 9.6 with the concomitant appearance of a new band at 1951 cm$^{-1}$. These two bands are assigned to two $\nu_{CO}$ stretching modes. Moreover, in $D_2O$ (pD 9.5), the frequency of the band at 1930.5 cm$^{-1}$ shifts to 1929.5 cm$^{-1}$. H−D isotopic shifts have been reported for the IR $\nu_{CO}$ of both CCP−CO (2 cm$^{-1}$) (*22*) and two forms of HRPC−CO (2.5 cm$^{-1}$ for form I and 1 cm$^{-1}$ for form II) (*23*).

Figure 4 shows a plot of $\nu_{FeC}$ versus $\nu_{CO}$ frequencies for the CO adducts of CIP−CO compared with those observed for CCP and HRPC, as reported in Table 1. HRPC at pH 6 exhibited two conformers (*5*). In form I of HRPC, the O atom of the bound CO interacts with the positively charged guanidinium group of the distal Arg via a H-bond. In the second HRPC−CO conformer (i.e., form II), the O atom of the bound CO molecule mainly interacts with the distal His

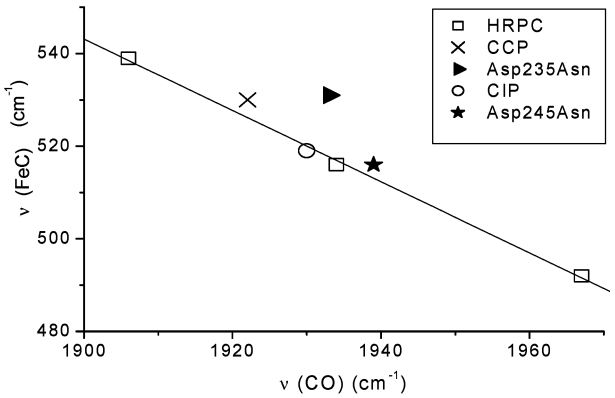


FIGURE 4: Plot of the $\nu_{FeC}$ vs $\nu_{CO}$ frequencies observed at acidic pH in the CO complexes of CIP (○), HRPC (□), CCP (×), and the proximal mutants Asp245Asn-CIP (★), and Asp235Asn-CCP (triangle pointing to the right). The line was obtained by fitting the data for HRPC at pH 6 (forms I and II) and pH 3 (see the text). The frequencies are listed in Table 1.

via a H-bond. HRPC at pH 3 (*24*) exhibited both a five-coordinate and a six-coordinate complex, this latter showing almost no interactions with the distal amino acids. The line shown in the plots in Figures 4, 6, 9, and 10 is obtained by fitting the vibrational frequencies of HRP form I, HRP form II, and six-coordinated HRPC−CO at pH 3, which we consider a reference set for all peroxidases. The CCP−CO adduct at pH 6 exhibited only one conformer characterized by vibrational frequencies corresponding to a weaker interaction with CO than in form I of HRPC. Therefore, it was assigned to a molecule of CO which is H-bonded to the distal Arg via a water molecule (*6*, *25*), as observed in the X-ray structure of the CCP−CO complex (*26*). In CCP at alkaline pH, the interaction between the bound CO and the distal pocket is weakened as suggested by the upshift of the $\nu_{CO}$ frequency and the downshift of the $\nu_{FeC}$ frequency, as compared to the acid form (*6*, *25*). On the contrary, for HRPC broad bands in both the IR and RR spectra were observed at 1933 and 530 $cm^{-1}$, respectively (*5*, *27*−*29*). They were tentatively assigned to the overlap of two conformers in which the CO interacts with Arg or $H_2O$ (*5*). This structural pH-dependent alteration corresponds to the proton-linked behavior of the CO dissociation process in both HRPC and CCP, in which the rate constants increase going from acid to alkaline pH by 4-fold in the former and by 1 order of magnitude in CCP (*7*, *19*).

Binding of CO to CIP produced different conformers, at pH 6 and 10. The conformer at pH 6 shows frequencies (519 and 1930.5 $cm^{-1}$) very close to those of form II of HRPC−CO (Figure 4). Therefore, it is assigned to CO H-bonded directly to the distal His (His55). H-Bonding from His55 to CO is geometrically favorable, as judged from the X-ray structure of ferric CIP (*11*), since $N_\epsilon$ of the distal His is in a nearly axial position ~6 Å above the Fe atom, very similar to $N_\epsilon$ of the distal His in HRPC. Moreover, the deuterium isotopic shift of the $\nu_{CO}$ stretch can be considered as further evidence for the existence of a H-bond to the carbonyl group, as previously found for other peroxidases (*22*, *23*). Therefore, we conclude that in CIP−CO at pH 6 the $N_\epsilon$ atom of the His55 residue is protonated and the O atom of the bound CO forms an almost linear H-bond with this N atom.

At pH 10, frequencies of 503 and 1951 $cm^{-1}$ of the other conformer suggest that CO is not H-bonded but only experiences polar interactions as in the alkaline CO complex of CCP. This feature is in close agreement with the pH dependence of the rates for CO dissociation in CIP−CO. The rate of CO dissociation increases with increasing pH, and it is coincident with the conversion of the CO complex from the acidic to the alkaline form. In fact, the occurrence of a H-bond with the distal His55 at pH 6 is associated with a decrease in the rate of CO dissociation, which is more than 100-fold slower than at alkaline pH, where the H-bond is not present (Table 1). It is interesting to note that at pH 6 the wt CIP−CO dissociation rate constant ($4.5 \times 10^{-5}$ $s^{-1}$) is similar to that of HRPC−CO [$7.2 \times 10^{-5}$ to $1.1 \times 10^{-4}$ $s^{-1}$ (*19*, *20*)] and recombinant CCP(MI)−CO [$7.0 \times 10^{-5}$ $s^{-1}$ (*7*)], suggesting only minor differences in the overall strength of the H-bonds between the CO and distal amino acids in these proteins. On the other hand, at alkaline pH the off rate constant displayed by CIP−CO is significantly faster ($6.3 \times 10^{-3}$ $s^{-1}$) than for HRPC−CO ($4 \times 10^{-4}$ $s^{-1}$) and CCP(MI)−CO ($8.0 \times 10^{-4}$ $s^{-1}$), indicating that the distal side of the heme pocket in CIP−CO is different from HRPC and appears to be more open or flexible.

*Asp245Asn Mutant.* The substitution of Asp245 with Asn causes small changes in the vibrational signature of the CO adduct compared to that of wt CIP. The $\nu_{FeC}$ frequencies are almost identical (Table 1), whereas the corresponding $\nu_{CO}$ bands [1939.5 and 1959 $cm^{-1}$ at acidic (pH 6) and alkaline pH, respectively] are at higher wavenumbers than those of wt CIP−CO. A similar effect was previously reported for the corresponding Asp235Asn mutant of CCP(MI) (*6*). These small changes are revealed by the slightly positive deviation from the fitting curve in Figure 4 seen for the Asn235 and Asn245 mutants. It is well-known that the proximal ligand influences CO binding to the heme as a result of competition for the empty Fe $d_z^2$ orbital and increases the responsiveness of $\nu_{FeC}$ to the back-bonding effect (*30*). Therefore, the changes observed for the Asp mutants of both CCP−CO and CIP−CO can be ascribed to a trans-ligand effect deriving from the weakening of the imidazolate character of the proximal His, as the H-bond of Asn with His is much weaker than the H-bond of Asp (*6*, *18*). The positive deviation from the linear correlation, therefore, implies a reduced electron density of the proximal imidazole ligand and is consistent with the very low Fe−His frequency, 205 $cm^{-1}$, seen for the ligand-free $Fe^{2+}$ CCP and CIP proteins (*6*, *18*). Such a reduced electron density appears to have a small effect on the rate of CO dissociation, since the Asp245Asn mutant displays a slightly faster rate than wt CIP at pH 6 (Table 1), but the same rate as wt CIP at alkaline pH. This clearly indicates that the trans-ligand effect of a weaker proximal H-bond is very limited except when CO is H-bonded to the distal His. A similar behavior is observed in the case of CCP, since at both pH 6 and 9 the Asp245Asn mutant displays values for the CO dissociation rate constant very similar to those shown by wt CCP (*7*).

*Arg51 Mutants.* The vibrational spectra of Arg51 mutants are markedly different from those of wt CIP when complexed with CO. Moreover, the substitution of Arg51 has some effect on the rates of CO dissociation, suggesting that this residue plays a role in the dynamics of the CO dissociation pathway. In fact, all Arg51 mutants display an approximately 10−15-fold increase of the rate for CO dissociation at pH 6 with respect to wt CIP−CO, the effect being fairly similar

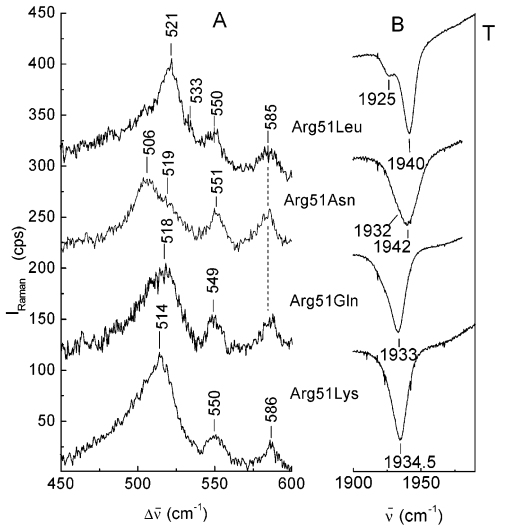


FIGURE 5: (A) RR spectra of the complexes of the Arg51 CIP mutants at pH 6 with $^{12}$CO. The spectra are measured with an excitation wavelength at 413.1 nm and a spectral resolution of 5 cm$^{-1}$. The integration times (from top to bottom) were 29, 25, 20, and 10. (B) Corresponding IR spectra at pH 6. Experimental conditions as described in the legend of Figure 3B.

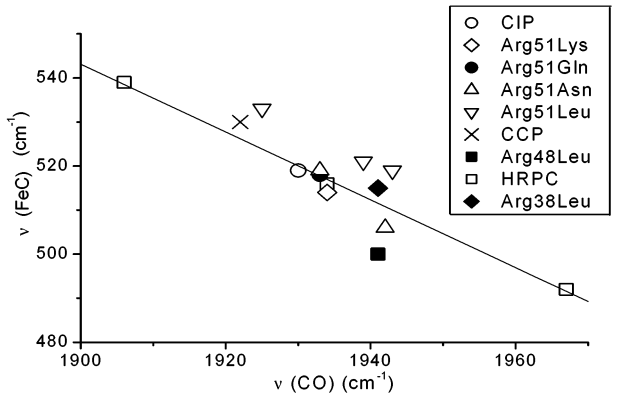


FIGURE 6: Plot of the $\nu_{FeC}$ vs $\nu_{CO}$ frequencies observed at pH 6 in the CO complexes of the Arg51 CIP mutants: Arg51Lys (◇), Arg51Gln (●), Arg51Asn (△), and Arg51Leu (▽). The points of CIP (○), HRPC (□), CCP (×), Arg38Leu HRPC (■), and Arg48Leu CCP (◆) are reported for comparison. The line is the same as in Figure 4. The frequencies are listed in Table 1.

in Arg51Lys, Arg51Asn, Arg51Gln, and Arg51Leu (see Table 1).

Panels A and B of Figure 5 compare the RR and IR spectra of the CO complexes of the Arg51 mutants at pH 6. It can be seen that replacing the distal Arg with either Lys or Gln does not markedly alter the vibrational signatures of the FeCO, despite the faster CO dissociation rate constant observed at pH 6 in Arg51Lys (∼12-fold) and Arg51Gln (∼16-fold) (see Table 1). For both mutants, only one form is observed with vibrational signatures similar to those of the wt CIP−CO complex (Table 1).

On the other hand, the spectra of the Asn and Leu mutants, both with shorter side chains, reveal the presence of many conformers. Fitting the spectra of the Arg51Asn−CO adduct yields two $\nu_{FeC}$ bands at 519 and 506 cm$^{-1}$ and two $\nu_{CO}$ bands at 1932 and 1942 cm$^{-1}$ (IR). On the basis of their relative intensities and frequencies (Table 2), two conformers are identified. The less abundant species is similar to that of CIP at pH 6 and characterized by $\nu_{FeC}$ and $\nu_{CO}$ stretches at 519 and 1932 cm$^{-1}$, respectively. In the other form, the $\nu_{FeC}$ decreases to 506 cm$^{-1}$ and the $\nu_{CO}$ increases to 1942 cm$^{-1}$. The occurrence of two conformers is consistent with the observation that Arg51Asn displays biphasic dissociation kinetics, indicating that the equilibrium between them is very slow. The most abundant (presumably characterized by $\nu_{FeC}$ at 506 cm$^{-1}$ and $\nu_{CO}$ at 1942 cm$^{-1}$) shows an approximately 17-fold faster dissociation rate with respect to wt CIP−CO. The second conformer (characterized by a $\nu_{FeC}$ at 519 cm$^{-1}$ and a $\nu_{CO}$ at 1932 cm$^{-1}$) shows a slower dissociation rate with a value similar to that observed for wt CIP at pH 6 (see Table 1). Therefore, Arg51Asn displays two CO binding modes at pH 6, one presumably H-bonded to His55, as in wt CIP, and the other interacting more weakly with the surroundings, although not as weakly as wt CIP at pH 10.0.

At pH 6, the Arg51Leu−CO complex also shows two conformers, characterized by $\nu_{FeC}$s at 533 and 521 cm$^{-1}$ and $\nu_{CO}$s at 1925 and 1940 cm$^{-1}$, respectively. However, a detailed study of the CO adduct between pH 4 and 10 revealed many peculiar characteristics not observed in the wt protein or in any other CIP mutant. First, the electronic absorption spectrum is pH-sensitive (data not shown), and the maxima of the bands red shift with increasing pH. In particular, the Soret band goes from 423 nm at pH 4, to 424 nm at pH 5, to 425 nm from pH 6 to 9. At pH 10, a blue shift of 1 nm is observed. This latter blue shift, very similar to that previously observed for CCP and selected mutants, including the distal Arg, indicates the conversion of the CO complex from the acidic to the alkaline form (*7*). At pH 4, the strongest IR band is observed at 1943 cm$^{-1}$. The band frequency decreases to 1940 cm$^{-1}$ at pH 5 and to 1938.5 cm$^{-1}$ at alkaline pH. It was not possible to obtain RR spectra at a pH lower than 5 due to the instability of the protein. However, at pH 5, the strongest RR band is observed at 519 cm$^{-1}$. This band upshifts by 2 cm$^{-1}$ at pH 6 and then remains unchanged up to pH 10.0 (data not shown). The other weak bands, at 533 cm$^{-1}$ (RR) and 1925 cm$^{-1}$ (IR), remain unchanged over the entire pH range. Nevertheless, they are assigned to the vibrational frequencies of the bound CO on the basis of isotopic sensitivity to $^{13}$CO (Table 1). For Arg51Leu at pH 6, one CO dissociation rate constant (3.8 × 10$^{-4}$ s$^{-1}$) that is ∼8-fold faster than in wt CIP−CO is observed. This indicates the presence of only one conformer corresponding to the most abundant form observed in the vibrational spectra. Alternatively, unlike for the case of Arg51Asn (see above), such a result might be consistent with the existence of different conformers in an equilibrium characterized by a relaxation rate that is faster than the CO dissociation rate constant itself.

In contrast to these results, the corresponding mutants of CCP (Arg48Leu−CO) (*6*) and HRPC (Arg38Leu−CO) (*5*) were very sensitive to this mutation, since the form characterized by the CO molecule H-bonded to the distal Arg disappeared. In particular, for CCP which shows only this conformer, the Arg38Leu mutant is characterized by a CO form with a marked decrease in the extent of back-donation with respect to the wt protein (Table 1 and Figure 6). Moreover, the CO dissociation rate enhancement with respect to the wt (∼20-fold at pH 6) is much more marked than that observed for Arg51Leu CIP with respect to wt CIP (∼8-fold). This most likely results from the interaction between the charged guanidinium group of the distal Arg with the

bound CO in CCP, but not in CIP.

Figure 6 shows the plot of the $\nu_{FeC}$ versus $\nu_{CO}$ frequencies for the CO adducts of distal Arg51 mutants of CIP, CCP, and HRPC at pH 6. The CO adducts of the mutants with polar side chains such as Gln (which contains an $N_\epsilon$ atom like Arg) and Lys (which is comparable in charge to Arg) have frequencies very close to those of CIP−CO. The same result is found for one conformer of the Arg51Asn−CO adduct, although the most abundant form of the Arg51Asn−CO complex shows a decreased degree of back-bonding. This weaker polar interaction with CO is possibly a consequence of the side chain of Asn being shorter than that of Gln.

When the distal Arg is replaced with the shorter aliphatic residue Leu, three conformers are found that are all positioned above the regression line. As concluded for the Asp245Asn mutant, a weakening of the proximal ligand can be inferred. This is again in agreement with a previous study of the ferric and ferrous Leu51 mutant which revealed a weakening of the Fe−Im bond (*14*). Two of the conformers have very close $\nu_{FeC}$ frequencies (519 and 521 $cm^{-1}$). The corresponding $\nu_{CO}$ frequencies (1938.5 and 1943 $cm^{-1}$) were obtained by fitting IR spectra at various pH values from 4 to 10 (data not shown). This data analysis indicated that the transition from one conformer to the other occurs with a p$K_a$ of approximately 5. Since the frequency separation of the $\nu_{CO}$ band maxima is small compared to the bandwidth, the band appears to shift with pH without a change in shape. A similar behavior was previously observed for the CO adduct of bovine heart myoglobin (*31*). These two conformers of the Arg51Leu CIP mutant show frequencies very similar to those of the pH 6 form of wt CIP−CO complex (Table 1), and they possibly have CO H-bonded to the distal His like wt CIP−CO.

The third conformer of the Arg51Leu−CO adduct (characterized by IR and RR frequencies of 1925 and 533 $cm^{-1}$, respectively), observed in the pH range of 4−10, is intriguing. This is shifted significantly on the back-bonding correlation plot toward the region of the complexes where the distal polar interactions are strong (e.g., HRP form I), although the distal Arg is replaced with the apolar side chain of Leu. The increased level of back-bonding compared to that of native CIP suggests a stronger interaction between the bound CO and a distal residue, and is also in agreement with the slower rate of CO dissociation at alkaline pH ($4.2 \times 10^{-5}$ $s^{-1}$). This conformer of the Arg51Leu−CO adduct, which is less populated and whose relative abundance is unaffected by pH changes between 4 and 10, could result from a conformational change induced by the mutation which, involving helix B, might favor a better interaction between the bound CO and the distal His. This change could be related to the weakening of the proximal Fe−Im bond resulting from the Arg to Leu mutation (*14*).

At alkaline pH, all the Arg51 mutants show only one conformer with vibrational signatures very similar to those of the wt protein at alkaline pH (see Table 1), with the exception of the Asn mutant characterized by a RR $\nu_{FeC}$ of 495 $cm^{-1}$. This band appears already at pH 6 with lower intensity (Table 2). At pH >10, all the mutants became unstable and showed the presence of an open form characterized by a $\nu_{FeC}$ of ∼490 $cm^{-1}$ (data not shown). However, the p$K_a$ of the alkaline transition appears to be changed in the Arg51 mutants, compared to the wt. The bands of the

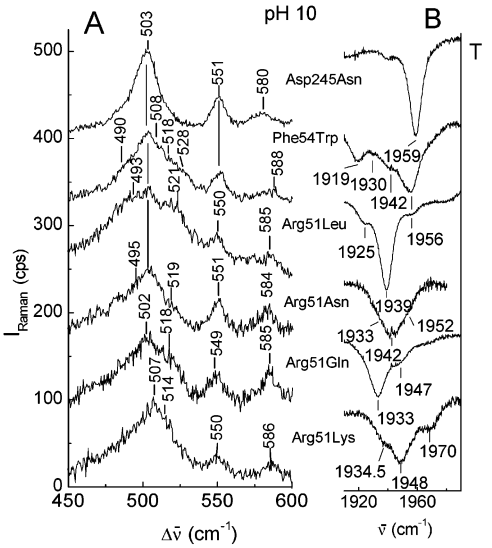


FIGURE 7: (A) RR spectra of the complexes of wt CIP and its mutants under investigation at pH 10 with $^{12}CO$. The spectra are measured with an excitation wavelength of 413.1 nm and a spectral resolution of 5 $cm^{-1}$. The integration times (from top to bottom) were 15, 20, 25, 50, 35, 8, and 20 s/0.5 $cm^{-1}$. (B) Corresponding IR spectra at pH 10. Experimental conditions were as described in the legend of Figure 3B.

acid forms are still clearly observed at pH 10 in all the Arg51 mutants, even appearing as the predominant form in the RR and IR spectra of the Arg51Leu variant (Figure 7) and thus indicating a higher p$K_a$ value. It must be underlined that CO is able to displace the $N_\epsilon$ atom of the amino group of Lys which is bound to the Fe atom in both the ferric and ferrous forms at alkaline pH (*14*). However, this mutant showed already at pH 9 a noticeable IR band at 1970 $cm^{-1}$, which increases in magnitude at pH 10, probably due to an open form as a consequence of partial unfolding or denaturation of the protein. The corresponding RR band is not clearly observed, being overlapped with a porphyrin mode at ∼490 $cm^{-1}$ (*32*).

At alkaline pH, the kinetics of CO dissociation from the Arg51 mutants always display a biphasic character, suggesting the existence of (at least) two conformers, which slowly interconvert, even though one is predominant. Arg51Asn displays two CO binding modes, one being similar to the form observed at pH 6 and the other having a higher CO dissociation rate ($1.6 \times 10^{-3}$ $s^{-1}$). This latter form has a rate almost identical to that observed for the Arg51Lys mutant ($1.8 \times 10^{-3}$ $s^{-1}$). On the other hand, the other species of the Arg51Lys mutant has a much greater CO dissociation rate ($1 \times 10^{-2}$ $s^{-1}$), even higher than that for wt CIP−CO at alkaline pH (Table 1). Such a high dissociation rate suggests that this species corresponds to the open form observed in the vibrational spectra.

Arg51Leu displays a biphasic character but with a different behavior since at pH 10 the predominant conformer has a CO dissociation rate ($2.5 \times 10^{-4}$ $s^{-1}$) closely similar to that observed at pH 6. Therefore, we assign this CO dissociation rate to the acid conformer characterized by the vibrational bands at 1938.5 and 521 $cm^{-1}$ which is the predominant form at pH 10 (see Figure 7 and Table 1). The second dissociation rate constant is ∼17-fold lower ($4.2 \times 10^{-5}$ $s^{-1}$) than the other, with a value very similar to that of wt CIP−CO at pH 6 (see Table 1). It is assigned to the Arg51Leu−CO

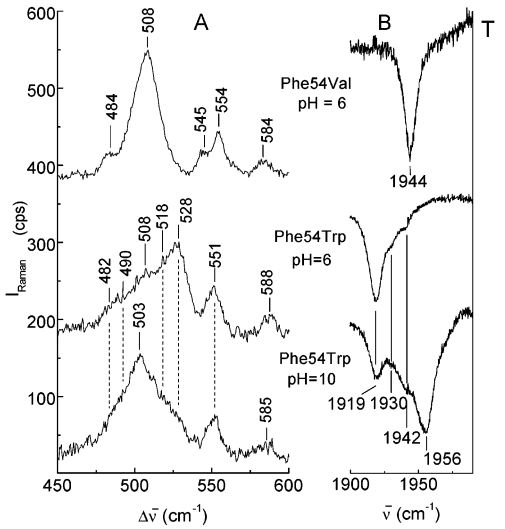


FIGURE 8: (A) RR spectra of the complexes of the Phe54 CIP mutants at pH 6 and 10 with $^{12}$CO. The spectra are measured with an excitation wavelength of 413.1 nm and a spectral resolution of 5 cm$^{-1}$. The integration times (from top to bottom) were 10, 80, and 20 s/0.5 cm$^{-1}$. (B) Corresponding IR spectra. Experimental conditions were as described in the legend of Figure 3B.

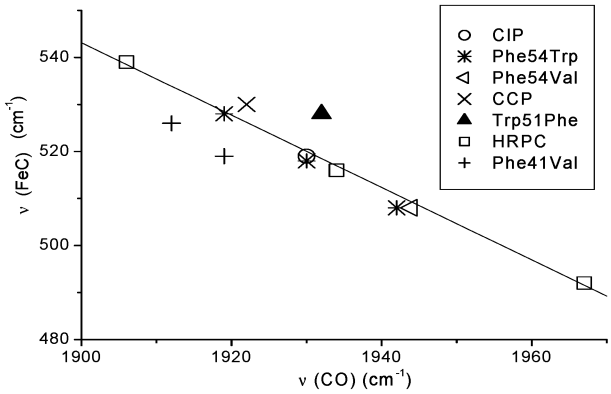


FIGURE 9: Plot of the $\nu_{FeC}$ vs $\nu_{CO}$ frequencies observed at pH 6 in the CO complexes of Phe51CIP mutants: Phe54Val (triangle pointing to the left) and Phe54Trp (∗). The points of CIP (○), HRPC (□), CCP (×), Phe41Val HRPC (+), and Trp51Phe CCP (▲) are reported for comparison. The line is the same as in Figure 4. The frequencies are listed in Table 1.

adduct observed between pH 4 and 10 (see above). The amount of the actual alkaline form of the Arg51Leu mutant characterized by the vibrational bands at 1956 and 503 cm$^{-1}$ appears to be negligibly small to be observed by kinetic measurements.

In conclusion, in a previous work (*14*), it has been demonstrated that the H-bond capability of the residue in position 51 influences the occupancy of the water molecules in the distal cavity which orchestrates the H-bond network of the distal cavity and the ability to form stable complexes between anionic ligands and the heme Fe atom. The presence in all the Arg51 mutants of a form with CO vibrational signatures similar to that of the CIP−CO adduct at pH 6 confirms that the positively charged guanidinium group does not directly interact with the bound CO via a H-bond. However, the spectroscopic data and the CO dissociation kinetics clearly show that the Arg residue is important for CO binding since the charge location, size, and H-bonding capability of the residue at position 51 modulate the back-bonding and the CO dissociation rate.

*Phe54 Mutants.* Mutation of the distal Phe54 to Val or Trp gave very different results (Figure 8A,B). At pH 6, the Phe54Val−CO adduct exhibits only one form characterized by $\nu_{FeC}$ and $\nu_{CO}$ bands at 508 and 1944 cm$^{-1}$, respectively, whereas the Phe54Trp−CO adduct exhibits many conformers. Its IR spectrum (Figure 8B) is characterized by three $\nu_{CO}$ bands at 1919, 1930, and 1942 cm$^{-1}$. On the basis of a band-fitting analysis of the RR spectra, the corresponding $\nu_{FeC}$ bands are identified at 528, 518, and 508 cm$^{-1}$, respectively (Figure 8A). At pH 10, a new form appears at 503 and 1956 cm$^{-1}$, with the concomitant decrease in magnitude of the bands observed at pH 6. The Phe54Trp mutant displays biphasic dissociation kinetics at both acidic and alkaline pH, suggesting that different conformers are in an equilibrium characterized by a relaxation rate that is faster than the CO dissociation rate constant itself. However, it is the only mutant which at pH 6 shows a conformer with a significantly smaller dissociation rate ($9.1 \times 10^{-6}$ s$^{-1}$) than the wt protein. The other dissociation rate ($7.6 \times 10^{-5}$ s$^{-1}$) is larger than that found for wt CIP. At alkaline pH, one species, corresponding to the alkaline form, has a CO dissociation rate that is ∼10-fold greater than at pH 6 ($3.5 \times 10^{-4}$ s$^{-1}$) which is more than 1 order of magnitude greater than that of the corresponding alkaline form of wt CIP, but very close to the value found for the alkaline form of CCP(MI) (*7*). The other CO dissociation rate attains a value similar to that measured at pH 6, since the acid forms are still present at a relatively high level as judged from the vibrational spectra (Figure 8).

The plot of the $\nu_{FeC}$ versus $\nu_{CO}$ frequencies for the CO adducts of the Phe54 mutants at pH 6 is shown in Figure 9. Replacement of Phe54 with Val weakens the interaction between the bound CO and the distal His unlike the corresponding mutant of HRPC (Phe41Val) (see Table 1). In that case, the mutation weakened the interaction between the bound CO and the distal Arg, without markedly affecting its interaction with the distal His (*33*). HRPC and CIP also give very different results upon substitution of distal Phe with Trp. In HRPC, which is characterized by a distal heme cavity that is smaller than those of other peroxidases (*12*), the extreme steric hindrance generated by the bulky Trp residue prevents immediate binding of CO, and the CO adduct is formed only after a major rearrangement of the distal pocket giving rise to an open form (*33*). On the contrary, in CIP the Phe54Trp−CO adduct shows three different conformers. The most abundant form lies significantly higher on the back-bonding correlation plot than the corresponding form of CIP−CO. We suggest that this form is due to the formation of an additional H-bond to the ligand via the $N_\epsilon$ atom of the indole ring. In fact, this conformer lies very close to that of wt CCP−CO (Figure 9), the X-ray structure of which showed a bound CO H-bonded to both the distal Arg and Trp via water molecules (*26*). Accordingly, this interpretation suggests that the CO dissociation rate of Phe54Trp CIP at pH 6 is significantly lower (∼5-fold) for the predominant conformer with a $\nu_{FeC}$ at 528 cm$^{-1}$ than for wt CIP (point 5, Table 1).

A second conformer of the Phe54Trp−CO adduct is similar to the wt protein, and the third form is similar to the Phe54Val−CO complex. Therefore, it appears that the mutation of Phe to Trp is also able to induce a change in

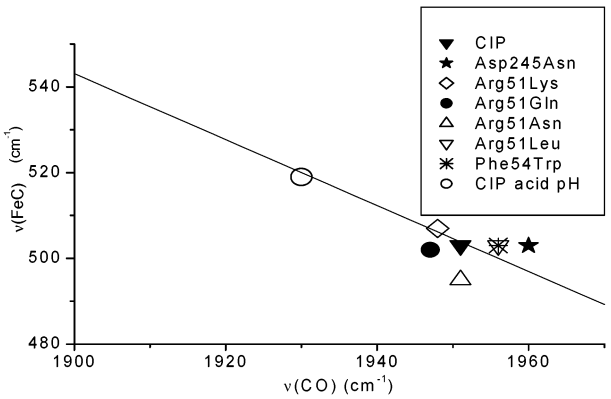


FIGURE 10: Plot of the $\nu_{FeC}$ vs $\nu_{CO}$ frequencies observed at alkaline pH in the CO complexes of CIP (▼) and its mutants under investigation: Asp245Asn (★), Arg51Lys (◇), Arg51Gln (●), Arg51Asn (△), Arg51Leu (▽), and Phe54Trp (∗). The point of CIP at acidic pH (○) is reported for comparison. The line is the same as in Figure 4. The frequencies are listed in Table 1.

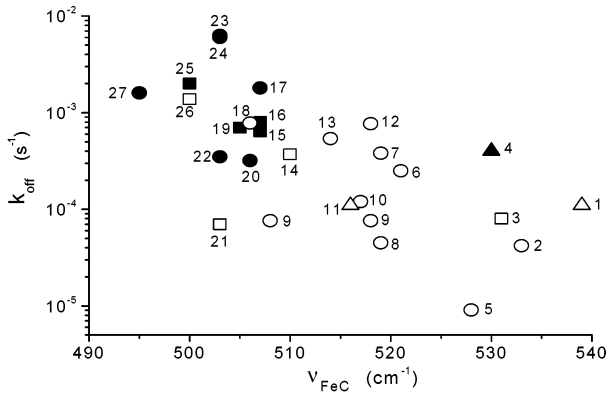


FIGURE 11: Experimental values of $k_{off}$ and $\nu_{FeC}$ frequency in CO adducts of ferrous CIP and selected mutants (○ and ●), CCP and selected mutants (□ and ■), and HRPC and selected mutants (△ and ▲). The empty symbols are for acidic pH, and the filled symbols are for alkaline pH. The frequencies and $k_{off}$ values are reported in Table 1: (1) HRPC form I, (2) Arg51Leu CIP, (3) Asp235Asn CCP, (4) HRPC, (5) Phe54Trp CIP, (6 and 7) Arg51Leu CIP, (8) CIP and Arg51Asn CIP, (9) Phe54Trp CIP, (10) Asp245Asn CIP, (11) HRPC form II, (12) Arg51Gln CIP, (13) Arg51Lys CIP, (14) Arg48Lys CCP, (15) Arg48Lys CCP, (16) CCPMI, (17) Arg51Lys CIP, (18) Arg51Asn CIP, (19) Asp235Asn CCP, (20) Arg51Asn CIP, (21) CCPMI, (22) Phe54Trp CIP, (23) CIP, (24) Asp245Asn CIP, (25) Arg48Leu CCP, (26) Arg48Leu CCP, and (27) Arg51Asn CIP.

the distal cavity, probably by varying the position of the distal His and, therefore, weakening the H-bond to CO. These forms most likely correspond to the species characterized by a dissociation rate constant of $0.76 \times 10^{-4}$ s$^{-1}$. It is noteworthy that the reverse mutation in CCP, i.e., replacing Trp51 with Phe does not markedly affect the vibrational signatures of the bound CO in the protein (*6*). The different effect can be ascribed to the very different interaction between the bound CO and the distal residues in CCP and CIP, i.e., with the guanidinium group of Arg in CCP and with the distal His in CIP.

Figure 10 shows the plot of the alkaline forms of the CO adducts of wt CIP and its mutants. It can be seen that all the proteins have a similar back-bonding, the level of which is lower than for the pH 6 form of the CIP−CO complex. Therefore, it can be concluded that at alkaline pH the CO is not H-bonded but experiences only polar interactions as previously reported for CCP.

*CO Dissociation Rate versus $\nu_{FeC}$ Frequencies*. When log $k_{off}$ is plotted as a function of $\nu_{FeC}$ for CIP and the mutants described here, together with HRPC, CCP, and selected mutants (*7*) (Figure 11), the observed trend toward increasing $\nu_{FeC}$ and decreasing $k_{off}$ is consistent with a concomitant increased influence of local polarity on $\nu_{FeC}$. A similar result was also obtained previously with the direct and inverse correlation between the CO dissociation constant and the values for $\nu_{FeCO}$ and $\nu_{FeC}$, respectively, for sperm whale myoglobin and pig myoglobin mutants (*1*, *3*, *8*). The stronger the bond, the slower the dissociation rate constant. The increase in the rate of CO dissociation with increasing pH is coincident with the conversion of the CO complex from the acidic to the alkaline form defined on the basis of the pH-dependent changes in the frequencies of the $\nu_{FeC}$ and $\nu_{CO}$ stretching modes. Some discrepancies are observed in the plot. This is the case of the CO complexes of CCP(MI) (point 21) and its mutant Asp235Asn (point 3) which have similar rates of CO dissociation but very different $\nu_{FeC}$ stretching frequencies (*7*). A different situation is represented by HRPC at pH 6 for which a single dissociation kinetics is measured but two conformers (forms I and II) are observed in the vibrational spectra (points 1 and 11). This indicates a fast equilibrium between the two conformers.

The alkaline forms of the CO complexes of all proteins and variants are grouped in the region corresponding to a low $\nu_{FeC}$ frequency and a fast CO dissociation rate, in agreement with the conclusion that the interaction between the bound CO and the distal environment is very weak. Moreover, the acid forms of the mutants of CCP that are altered at Arg48 (□, points 14 and 26) also fall in this region, since the H-bond interaction between the CO and the positively charged guanidinium group is lost in the variants. The alkaline form of HRPC (▲) contrasts with alkaline forms of the CO complexes as it falls together with the adducts in which the CO experiences a H-bond interaction. In particular, in the central part of the plot, we found HRPC form II, wt CIP, and some of its variants, all having a H-bond interaction between the oxygen atom of the bound CO and the distal His. The highest values of $\nu_{FeC}$, and accordingly the smaller CO dissociation rate, are observed for HRPC form I, and the Asp235Asn variant of CCP which shows a strong back-donation due to the CO ligand H-bonded directly or via a water molecule with the distal Arg (*5*). One of the conformers of the Phe54Trp CIP and Arg51Leu CIP mutants falls in this region, suggesting that there is an effect of increased polarity on the $\nu_{FeC}$ as a consequence of a stronger H-bond interaction as compared to that of wt CIP.

We have also measured the CO binding equilibrium constant ($K_{co}$) of wt CIP at pH 6 ($6.4 \times 10^8$ M$^{-1}$) and pH 10 ($3.0 \times 10^7$ M$^{-1}$). At alkaline pH, $K_{co}$ is 1 order of magnitude lower than at pH 6; this effect, which perfectly mirrors the $k_{on}/k_{off}$ ratio at the two pH values, is related to a decrease by 1 order of magnitude for $k_{on}$ when the pH is lowered from 10 to 6 (unpublished data) and to a decrease by 2 orders of magnitude of $k_{off}$ over the same pH range (Table 1). Apart from that of the Asp245Asn mutant, the equilibrium constants are markedly affected by mutations (data not shown). However, as previously found for myoglobin (*8*), we did not find a direct correlation between the

effects induced by mutation (electrostatic and steric effects) and the change in $K_{co}$. Moreover, for most CIP mutants, the interpretation of the data is complicated by the existence of multiple conformers. In addition, a lack of correlation was found between $\nu_{FeC}$ (or $\nu_{CO}$) and the equilibrium constant $K_{co}$. A similar result was also obtained by Li and co-workers (*3*), who presented a correlation between rate and equilibrium constants for CO binding and $\nu_{CO}$ for sperm whale and pig Mb mutants.

The simplest explanation of these results is that only $k_{off}$ is correlated to the vibrational frequencies, since it is mainly related to the strength of the Fe−CO bond order, whereas $K_{co}$ is also influenced by other effects, namely, hydration of the distal cavity and steric hindrance that block access to the iron atom.

## CONCLUSIONS

The combination of the vibrational and kinetic data at alkaline pH allows us to conclude that the ferrous CIP−CO is characterized by a much more open cavity than the other peroxidases. In fact, the $k_{off}$ value for CIP at alkaline pH is 1 order of magnitude larger than for HRPC and CCP. The acid form of CIP−CO has a H-bond interaction with the distal His, very similar to form II in HRPC. However, despite the distal Arg being unable to interact directly with the CO ligand, as suggested also by its location in the crystal structure (*34*), the residue is important in determining the rate of dissociation in the acidic form of ferrous CIP−CO. When Arg51 is replaced with Leu, Lys, Asn, or Gln, the rate of CO dissociation for the acidic form is increased by 8-, 12-, 16-, or 17-fold, respectively, whereas in the alkaline CO complex, the influence of the Arg on the rate of the CO dissociation is almost negligible. The data presented here confirm previous results showing that in the case of the Arg51Leu mutant a more complex change in the cavity occurs which appears to involve both the distal and proximal sides of the heme, in agreement with the observed weakening of the proximal Fe−Im bond (*14*). This effect is peculiar to only CIP since no alteration was observed in the corresponding mutants of HRPC and CCP. Moreover, these results highlight the high sensitivity of the CO ligand as a probe for investigating the environment of the heme cavity.

Finally, the replacement of the distal Phe with Trp is able to create a new acid form characterized by a stronger H-bond interaction than in wt CIP. This form, which is similar to that found in wt CCP, corresponds to the formation of an extra H-bond between CO and the $N_\epsilon$ atom of the indole group. This interaction appears to be maintained in the alkaline form as judged by the rate of CO dissociation of the Phe54Trp−CO adduct, similar to the alkaline form of CCP, but decreased by ~6-fold with respect to the alkaline form of wt CIP.

## REFERENCES


1. Phillips, G. N. J., Teodoro, M. L., Smith, B., and Olson, J. S. (1999) *J. Phys. Chem. B 103*, 8817−8829.
2. Ray, G. B., Li, X.-Y., Ibers, J. A., Sessler, J. L., and Spiro, T. G. (1994) *J. Am. Chem. Soc. 116*, 162−176.
3. Li, T., Quillin, M. L., Phillips, G. N., Jr., and Olson, J. S. (1994) *Biochemistry 33*, 1433−1446.
4. Uno, T., Nishimura, Y., Tsuboi, M., Makino, R., Iizuka, T., and Ishimura, Y. (1987) *J. Biol. Chem. 262*, 4549−4556.
5. Feis, A., Rodriguez-Lopez, J. N., Thorneley, R. N. F., and Smulevich, G. (1998) *Biochemistry 37*, 13575−13581.
6. Smulevich, G., Mauro, J. M., Fishel, L. A., English, A. M., Kraut, J., and Spiro, T. G. (1988) *Biochemistry 27*, 5486-5492.
7. Miller, M. A., Mauro, J. M., Smulevich, G., Coletta, M., Kraut, J., and Traylor, T. G. (1990) *Biochemistry 29*, 9978−9988.
8. Springer, B. A., Sligar, S. G., Olson, J. S., and Phillips, G. N. J. (1994) *Chem. Rev. 94*, 699−714.
9. Abelskov, A. K., Smith, A. T., Rasmussen, C. B., Dunford, H. B., and Welinder, K. G. (1997) *Biochemistry 36*, 9453−9463.
10. Petersen, J. W. F., Kadziola, A., and Larsen, S. (1994) *FEBS Lett. 339*, 291−296.
11. Kunishima, N., Amada, F., Fukuyama, K., Kawamoto, M., Matsunaga, T., and Matsubara, H. (1996) *FEBS Lett. 378*, 291−294.
12. Gajhede, M., Schuller, D. J., Henriksen, A., Smith, A. T., and Poulos, T. L. (1997) *Nat. Struct. Biol. 4*, 1032−1038.
13. Finzel, B. C., Poulos, T. L., and Kraut, J. (1984) *J. Biol. Chem. 259*, 13027−13036.
14. Neri, F., Indiani, C., Welinder, K. G., and Smulevich, G. (1998) *Eur. J. Biochem. 251*, 830−838.
15. Neri, F., Indiani, C., Baldi, B., Vind, J., Welinder, K. G., and Smulevich, G. (1999) *Biochemistry 38*, 7819−7827.
16. Dalbøge, H., Jensen, E. B., and Welinder, K. G. (1992) Pat. Appl. WO 92/16634.
17. Smulevich, G., Feis, A., Focardi, C., and Welinder, K. G. (1994) *Biochemistry 33*, 15425−15432.
18. Smulevich, G., Neri, F., Marzocchi, M. P., and Welinder, K. G. (1996) *Biochemistry 35*, 10576−10585.
19. Coletta, M., Ascoli, F., Brunori, M., and Traylor, T. G. (1986) *J. Biol. Chem. 261*, 9811−9814.
20. Wittenberg, B. A., Antonini, E., Brunori, M., Noble, W., Jr., Wittenberg, J. B., and Wyman, J. (1967) *Biochemistry 6*, 1970−1974.
21. Heering, H. A., Jansen, M. A., Thorneley, R. N., and Smulevich, G. (2001) *Biochemistry 40*, 10360−10370.
22. Satterlee, J. D., and Erman, J. E. (1984) *J. Am. Chem. Soc. 106*, 1139−1140.
23. Smith, M. L., Ohlsson, P.-I., and Paul, K. G. (1983) *FEBS Lett. 163*, 303−305.
24. Smulevich, G., Paoli, M., De Sanctis, G., Mantini, A. R., Ascoli, F., and Coletta, M. (1997) *Biochemistry 36*, 640−649.
25. Smulevich, G., Evangelista-Kirkup, R., English, A., and Spiro, T. G. (1986) *Biochemistry 25*, 4426−4430.
26. Edwards, S. L., and Poulos, T. L. (1990) *J. Biol. Chem. 265*, 2588−2595.
27. Barlow, C. H., Ohlsson, P.-I., and Paul, K. G. (1976) *Biochemistry 15*, 2225−2229.
28. Holzbaur, I. E., English, A. M., and Ismail, A. A. (1996) *J. Am. Chem. Soc. 118*, 3354−3359.
29. Rodriguez-Lopez, J. N., George, S. J., and Thorneley, R. N. F. (1998) *J. Biol. Inorg. Chem. 3*, 44−52.
30. Vogel, K. M., Kozlowski, P. M., Zgierski, M. Z., and Spiro, T. G. (2000) *Inorg. Chim. Acta 297*, 11−17.
31. Shimada, H., and Caughey, W. S. (1982) *J. Biol. Chem. 357*, 11893.
32. Evangelista-Kirkup, R., Smulevich, G., and Spiro, T. G. (1986) *Biochemistry 25*, 4420−4425.
33. Heering, H. A., Smith, A. T., and Smulevich, G. (2002) *Biochem. J. 363*, 571−579.
34. Kunishima, N., Fukuyama, K., Matsubara, H., Hatanaka, H., Shibano, Y., and Amachi, T. (1994) *J. Mol. Biol. 235*, 331−344.


BI026203C